

# HYDROXYL INVESTIGATION IN ETHANOL FLAME USING PLANAR LASER INDUCED FLUORESCENCE (PLIF) AND EMISSION SPECTROSCOPY

**Maria Esther Sbampato, esther@ieav.cta.br**

Instituto de Estudos Avançados, Rod. dos Tamoios, Km 5,5 - São José dos Campos -SP - Brasil

**Luiz Gilberto Barreta, barreta@ieav.cta.br**

Instituto de Estudos Avançados, Rod. dos Tamoios, Km 5,5 - São José dos Campos -SP - Brasil

**Cristiane Aparecida Martins Andraus, cmartins@ita.br**

Instituto Tecnológico de Aeronautica, Praça Marechal Eduardo Gomes, 50 - São José dos Campos -SP - Brasil

**Natacha Alencar Januário, natachableh@gmail.com**

Instituto de Estudos Avançados, Rod. dos Tamoios, Km 5,5 - São José dos Campos -SP - Brasil

**Fernanda Rosa Diamantino, fer\_diamantino@yahoo.com.br**

Instituto de Estudos Avançados, Rod. dos Tamoios, Km 5,5 - São José dos Campos -SP - Brasil

**Leila Ribeiro dos Santos, leila@ieav.cta.br**

Instituto de Estudos Avançados, Rod. dos Tamoios, Km 5,5 - São José dos Campos -SP - Brasil

**Alberto Monteiro dos Santos, alberto@ieav.cta.br**

Instituto de Estudos Avançados, Rod. dos Tamoios, Km 5,5 - São José dos Campos -SP - Brasil

**Abstract.** *In this work planar laser induced fluorescence (PLIF) is used for relative concentration measurements of hydroxyl, or OH, which is an important short-living species, a chain carrier in combustion reactions along with O and H. The radical OH was investigated at partially premixed ethanol flames produced in a burner constructed in our laboratory. The ethanol was vaporized and the flames used mixtures of air and pure O<sub>2</sub> as oxidant. The flame temperatures at various flame heights were previously obtained through OH LIF experiments. Partially premixed flames reached temperatures between 1900 K and 2200 K. Emission distribution of excited OH radicals formed during the burning process were obtained with an ICCD camera. The experimental setup for PLIF consisted of a Nd-YAG pumped dye-laser, cylindrical lenses to produce a 300 μm thick and 30 mm high laser sheet and an ICCD camera. The emission technique does not allow the visualization of the internal flame structure of the three kinds of flames studied while PLIF images show significant differences among them.*

**Keywords:** *PLIF, OH radical, ethanol flame, emission spectroscopy*

## 1-INTRODUCTION

Laser induced-fluorescence (LIF) techniques are widely applied as diagnostic tools for combustion investigations where a detailed understanding of certain chemical reaction pathways is desired. They provide powerful methods for studies of combustion chemical reaction dynamics and flame structure (Bombac e Kappeli, 1999). LIF is a well-established sensitive technique for detecting population densities of molecules and/or atoms in specific quantum states and can be used to measure concentrations of the OH, NO, CH, and CN radicals. Eckbreth (1988) summarizes the development of different LIF methods and their application to the measurement of species concentration and temperature in combustion diagnostics.

LIF techniques, when carefully applied, are capable of measuring absolute concentrations of reactive species but this feature is not always essential. The mere detection of a particular species in a specific combustion environment may provide some insight into the chemistry of the process. Using two-dimensional LIF schemes (planar laser induced fluorescence - PLIF), it is possible to measure time-resolved relative spatial distribution of the species under investigation (Yang *et al.*, 2002). In the PLIF imaging experiment, the reactive flow is illuminated with a planar laser sheet delivered by a tunable laser. The laser light excites a species that is present in the flow, the excited species fluoresce and this fluorescence is detected with a intensified charge-coupled device (ICCD) camera.

### 1.1 LIF background

LIF involves exciting an atom or molecule to an excited quantum state with laser radiation and observing the resulting spontaneous radiation from the directly excited state or from nearby states that have been indirectly populated by collisions (Daily, 2000). The LIF signal,  $I_F$  can be related to specific properties, e.g. temperature,  $T$ , pressure,  $P$ , and concentrations of the molecules or atoms,  $\chi$ :

$$I_F = \frac{E\chi P}{SkT} f_J Bg \frac{A}{A+Q} \eta \quad 1.1$$

where,  $E$  is the energy of the laser source,  $S$  the interaction area between the laser sheet and molecules or atoms,  $k$  the Boltzmann constant,  $f_J$  the Boltzmann expression with rotational quantum number  $J$ ,  $B$  the Einstein coefficient,  $g$  the overlap integral,  $A$  the spontaneous emission rate,  $Q$  the quenching rate,  $\eta$  the fluorescence transfer efficiency of the ICCD,  $A/(A+Q)$  is so-called fluorescence producing efficiency.

In order to assure that only the LIF signal reaches the detector during the experiment, the choice of the excitation/detection strategy is very important. In combustion experiments, sources of elastic scattering may deflect the laser radiation toward the collection optics, resulting in signal contamination. The elastic scattering only occurs at the laser wavelength and the fluorescence occurs at the wavelength of all allowed transitions from the populated upper energy level and also from nearby levels populated through collisional energy transfer. If there is a spectral separation between part of the fluorescence signal and the original laser wavelength, it is possible to filter the parasite elastic laser scattering from the resulting fluorescence signal. The model of LIF operation depends on the specie under investigation.

Another important experimental choice is related to the particular rotational level,  $J$  that will be excited. If the quenching rate (proportional to  $T^{1/2}$ ), is not considered, the  $J$  which is least sensitive to temperature variations, can be expressed as:

$$J^2 + J - \left( \frac{k}{hcB_V} \right) \bar{T} = 0 \quad 1.2$$

where  $T$  is an average flame temperature and  $J$  the rotational number, whose population is least sensitive to temperature changes. Therefore, by judiciously selecting the initial level for excitation, namely  $J$ , the measurements become quite insensitive to temperature

## 1.2 Radicals in flames

Literature and several authors have been in search of flame and radical relationships. It is clear that the desire is to find, if possible, some linear and direct relation between both. PLIF technique gives some accurate information of combustion process, for example, the precious information about the determination of the position and the shape of the combustion reaction zone. The answers come with the radicals considered as "flame indicator species" (OH, CH, C<sub>2</sub>, CHO and others). These radicals are generated only in the combustion reaction zone in higher concentration. In fact, their concentrations may rise by powers of ten within distances of about 1mm or less. Martins et al. (2005) utilized the CHEMKIN 3.6 package (Kee et al., 2000) to investigate the kinetic behavior of the CH, C<sub>2</sub> and OH radicals. This work shows that the correlation between the C<sub>2</sub>/CH radicals and the temperature is stronger than that for the OH radical and the temperature. This suggests that the two first radicals represent a more precise signature of the reaction zone. In fact, the C carrying species are burnt up again and represent true flame indicators. However, the indicator OH is the most often used in PLIF measurements mainly due to its high concentration. Also, some authors (Mokaddem et al. 1994 and Nguyen and Paul, 1996) suggest that due to the superior relaxation time of OH (10<sup>-3</sup>s) compared with C<sub>2</sub> (10<sup>-7</sup>s) and CH (10<sup>-5</sup>s) this radical could survive along the flame region and still appear at the "end" of flames.

## 1.3 Emission imaging

Besides PLIF, time-average line-of-sight spontaneously emission imaging provides qualitative information about certain radicals produced by the combustion chemical reaction. The chemiluminescent emission, in general, may be interpreted as a signature of chemical reaction and can be used to delimit regions of reaction and heat release (McManus et al., 1995). The radioactive decay of excited species as the (0,0) band transitions of OH (A<sup>2</sup>Σ → X<sup>2</sup>Π), CHO (A<sup>2</sup>Π → X<sup>2</sup>A'), CH (A<sup>2</sup>Δ → X<sup>2</sup>Π) and C<sub>2</sub> (A<sup>3</sup>Π → X<sup>3</sup>Π) are mainly responsible for the chemiluminescence observed in the combustion of hydrocarbon fuels (Gaydon, 1974). However the chemical processes of excited species formation has not yet been definitely established. Imaging of the light emission of free radicals such as C<sub>2</sub><sup>\*</sup>, CH<sup>\*</sup> and OH<sup>\*</sup> are valuable in turbulent flames (here the asterisk indicates excited species). Experimentally, the flame chemiluminescence image is detected with a CCD or with an intensified CCD camera and delivered to a computer for further processing. Whereas the method remains essentially qualitative, it provides valuable information on combustion dynamics and is useful in studies of unstable and transient reactive flows.

## 1.4 OH-radical

The OH is an important radical in the chemistry of any combustion-related process containing hydrogen and oxygen species. In such systems, it is often measured using spectroscopic methods in the well-known A<sup>1</sup>Σ<sup>+</sup> - X<sup>2</sup>Π<sub>i</sub> electronic

system (Luque e Crosley, 1998, Dieke e Crosswhite, 1961). It is important to note that emission spectroscopy detects radicals produced in the electronic excited state ( $\text{OH}^*$ ) and PLIF experiments visualize non-excited OH radicals. It is known that the chemical mechanisms for the production of fundamental OH and excited  $\text{OH}^*$  radicals are different. The fraction of OH radicals that are in an electronically excited state is small (about 1000 times lower than the non-excited OH) and consequently the photon flux is relatively small. The intensity of the  $\text{OH}^*$  fluorescence signal is modified by the self-absorption of radiation by non-excited OH radicals and the amplitude of this effect is not easily interpreted in quantitative terms.

A good choice for OH-PLIF excitation/detection strategy is to excite the vibrational-rotational  $1 \leftarrow 0$  of the electronic transition  $A^1\Sigma^+ - X^2\Pi_i$  at 283 nm region and detect the fluorescence in the region of  $1 \leftarrow 1$  and  $0 \leftarrow 0$  vibrational-rotational transitions ( $\sim 304$  nm to 320 nm). According to equation 1.1, for the OH radical,  $J=8.5$  is almost constant for the temperature range of 1000~2600K, and  $J=5.5$  for the temperature range of 900~1700K and levels associated with these rotational quantum numbers may be selected for OH-LIF measurements. When the quenching rate is taken into account,  $J=5.5$  is found to be a good choice in the temperature range of 1500 K  $< T <$  3500 K (McManus et al., 1995).

The aim of this work is to study the  $\text{OH}^*$  and OH radicals distributions in three partially premixed vaporized ethanol/air/ $\text{O}_2$  flames employing PLIF imaging and emission imaging.

## 2. EXPERIMENTAL

A schematic of the experimental setup is shown in Fig. 1. The laser system consists of a Sirah pulsed dye-laser pumped by a Quanta-Ray Nd:YAG laser. The emitting laser pulse duration is 7 ns. Light from the Nd:YAG laser at a wavelength of 1064 nm passes through a frequency-doubling crystal producing 532 nm light which pumps the dye laser operated with Rhodamine 6G solution in ethanol. The dye laser outputs light at 566 nm regions, which is frequency-doubled by a KDP crystal producing laser radiation at the 283 nm regions. The dye laser radiation is narrowband ( $0.2 \text{ cm}^{-1}$ ) and wavelength tunable by the harmonic generation unit. This light excites transitions in the  $A\Sigma-X\Pi$  ( $1; 0$ ) band of OH radical. In this experiment, the OH radicals were excited at 283.906 nm ( $Q_1(9)+Q_2(8)$ ). The output beam of the dye laser is converted into a 300  $\mu\text{m}$  width and 30 mm heigh sheet at the flame position.. The sheet is produced with two cylindrical lenses ( $f=-300$  mm and  $f=+500$  mm). The laser energy is approximately 0.5 mJ per pulse that assures a linear regime. The image is acquired by a 1024 $\times$ 1248 pixel intensified CCD camera (Cooke Instruments, DICAM-PRO) and a 105 mm f/4.5 quartz NIKON camera lens. A Schot WG295 filter is placed in front of the lens to reject scattered residual 283 nm lights and a Schot UG5 filter is also used to eliminate visible light background. The detected light is the OH fluorescence at 310 nm region ( $A\Sigma-X\Pi$  ( $0; 0$ ) and  $A\Sigma-X\Pi$  ( $1; 1$ ) bands). The camera is held perpendicular to the excitation laser sheet direction. A Newport Model 818E-10-25F detector that collects the laser radiation after the flame monitors the laser energy during the experiment. The  $\text{OH}^*$  chemiluminescence images are obtained with the same experimental setup excluding the laser radiation

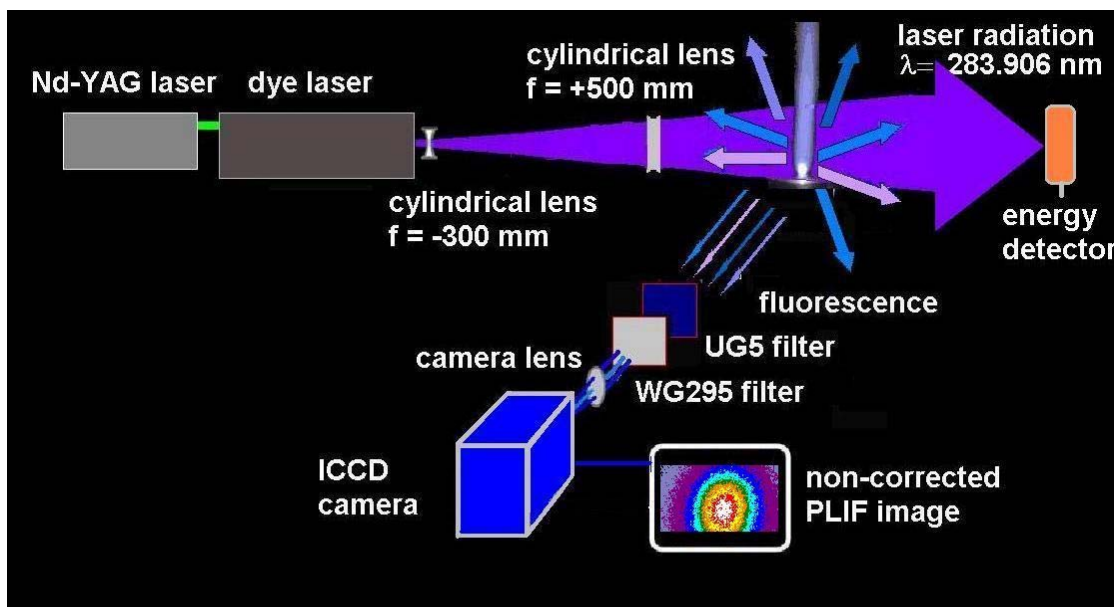


Figure 1. Experimental setup for OH PLIF and  $\text{OH}^*$  emission measurements in the ethanol flame.

The burner was constructed according to the design proposed by Lacava, 1995. It is a “y” type premixed burner; projected to burn liquid fuels but it can also be used with gases. The small chamber of the burner acts as an atomizer to produce small droplets when a liquid fuel is used and as a premixing chamber for gas fuels. Figure 2 shows the burner, with some details of the construction. The burner orifice can be varied. In these experiments, a 1.0 mm orifice diameter was used

In the present work, three vaporized ethanol/air/O<sub>2</sub> flames were studied. The conditions are shown in Tab. 1. The fuel, oxygen and airflow rates were measured with flow meters (COLE PARMER, FM012-10, FM023-92 and FM014-96 models, respectively). Ethanol was vaporized passing it through a copper coil heated by a heating tape (Fig. 2(b)).

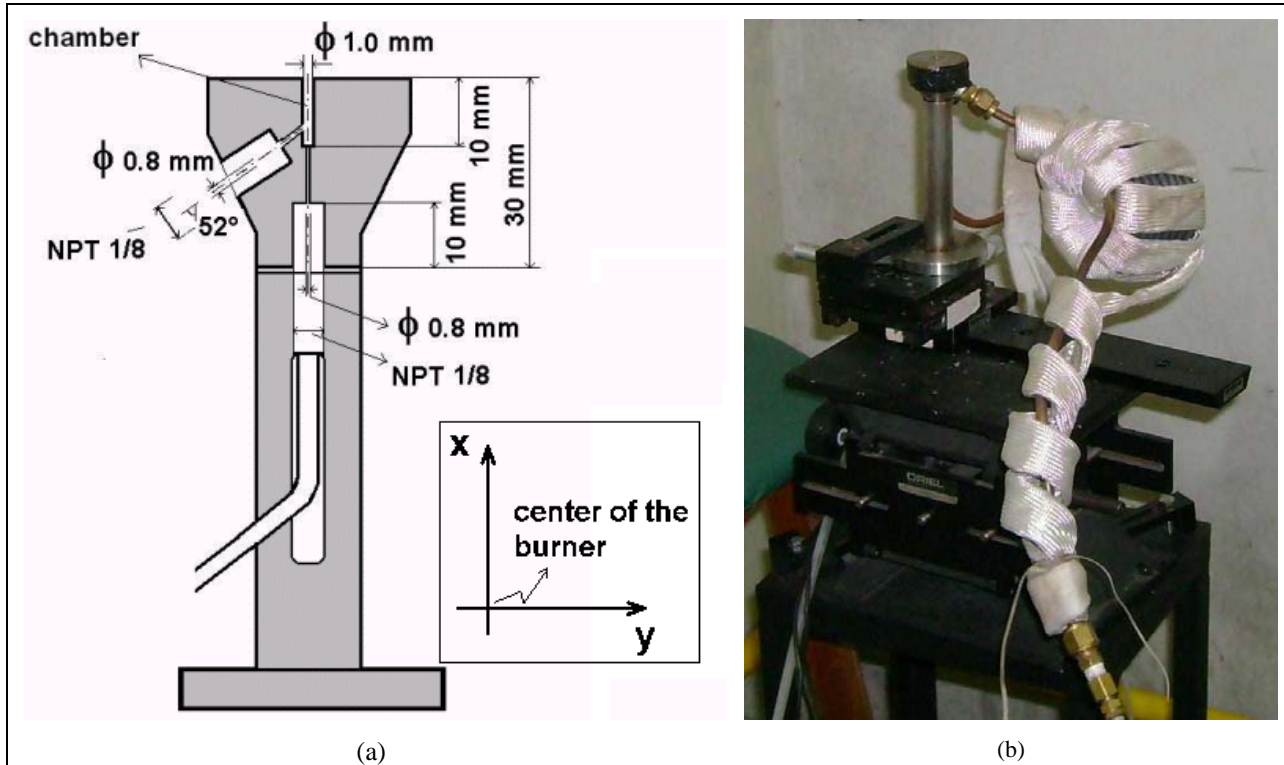


Figure 2. - Gas/liquid burner (a) Schematic design showing the coordinate system considerate in this work; (b) Photo.

The OH PLIF images were obtained at the center of the burner exit and at 5 different flame x-heights (each 20 mm high) using a jack facility, as shown in Fig. 2(b). As the laser beam is 30 mm high, there was an image superposition of about 10 mm. The camera conditions were: 140 ns exposure time, 25 loops for the  $\phi=2.4$  flame, 15 loops for the  $\phi=1.8$  flame and 12 loops for the  $\phi=1.5$  flame. The OH\* chemiluminescence was obtained employing an exposure time of 25  $\mu$ s and 120 loops for the  $\phi=2.4$  flame, 30 loops for the  $\phi=1.8$  flame and 20 loops for  $\phi=1.5$  flame. The PLIF beam profile correction (the laser beam presents a gaussian spatial energy profile that needs to be considerate in non-saturated PLIF-experiments) and image treatments were made employing software developed in MATHCAD.

Table 1 - Ethanol/air/O<sub>2</sub> flame conditions ( $\phi$  = equivalence ratio,  $\dot{m}_{fuel}$  = fuel mass flow rate,  $\dot{m}_{air}$  = air mass flow rate,

$\dot{m}_{O_2}$  = O<sub>2</sub> mass flow rate, Re = Reynolds number)

Flame	$\phi$	$\dot{m}_{fuel}$ (10 <sup>-6</sup> kg.s <sup>-1</sup> )	$\dot{m}_{air}$ (10 <sup>-6</sup> kg.s <sup>-1</sup> )	$\dot{m}_{O_2}$ (10 <sup>-6</sup> kg.s <sup>-1</sup> )
1	2.4	28.7	6.84	23.6
2	1.8	28.7	6.84	31.7
3	1.5	28.7	6.84	38.4

### 3. RESULTS AND DISCUSSION

Figure 3 shows the photos, the OH\* emission images and the OH-PLIF images for the three studied flames normalized in relation to the  $\phi = 1.5$  flame that presents the highest OH\* and OH concentrations. The results for the profile along the x-axis for the OH\* radical and OH radical are shown in Fig. 4a and Fig. 4b, respectively. The developed program to analyze the data considerate only the pixels intensities along the  $y \pm 0.5$  mm of the burner orifice.

Figure 5 shows the radial ( $y/d$ )  $\text{OH}^*$  distribution at some height downstream from the nozzle exit for the three flames obtained from the emission images. Figure 6 shows the  $\text{OH}$  radial distribution obtained from the PLIF images for the same flames.

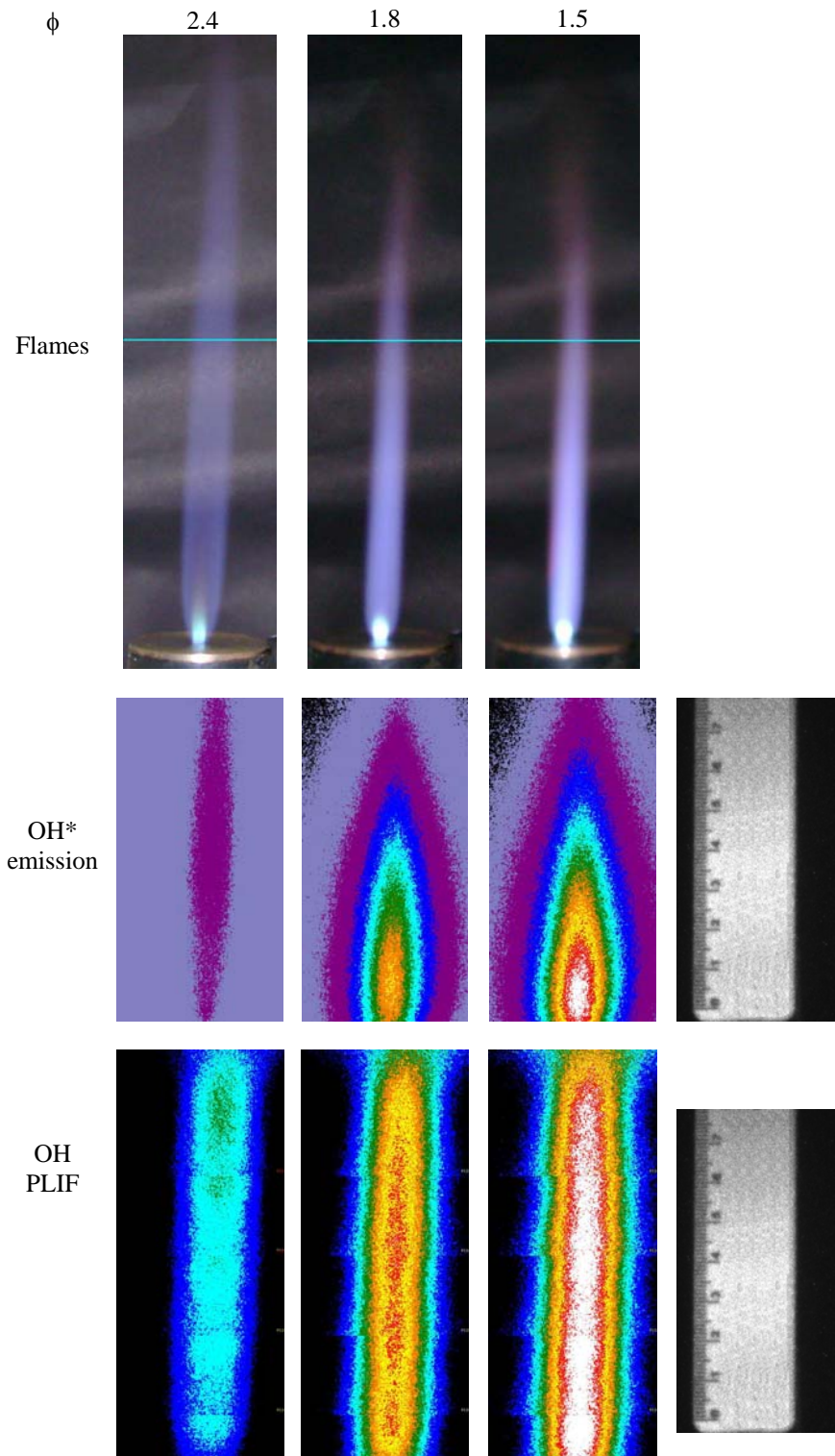


Figure 3. Photo, OH emission images and OH-PLIF images for the three studied flames. The data are normalized in relation to the  $\phi=1.5$  flame (maximum  $\text{OH}^*$  and OH concentration).

The PLIF measurements show a wider OH intensity profile at the x-location downstream of the nozzle exit than that obtained for OH\* thought emission images (Fig.4), and the same may be observed for the radial OH\* and OH distribution (Fig.5 and Fig. 6). This is expected since the LIF technique excites the ground state OH radicals, which may exist outside the reaction zone in the post-combustion gases. The emission technique only detects the natural chemiluminescence from the excited radicals formed in the combustion. Therefore, since there is no primary combustion in the post-combustion gases, the chemiluminescence intensity from OH\* radicals is lower there.

In the radial direction, the maximum OH\* intensity were observed at the center of the flame, and the same was observed for the OH intensities (PLIF measurements). In the x-direction, the maximum OH\* intensities were observed at:

$$\begin{aligned} x=44 \text{ mm}, \phi &= 2.4 \\ x=11 \text{ mm}, \phi &= 1.8 \\ x=7.5 \text{ mm}, \phi &= 1.5 \end{aligned}$$

Pela Fig. 4, observa-se que, para as chamas de  $\phi = 1.8$  e  $\phi = 1.5$ , a concentração de OH no estado fundamental aumenta a partir do queimador até aproximadamente 10 mm e, então, apresenta, uma queda suave até a altura de 90 mm. Para a chama mais rica ( $\phi=2.4$ ), a concentração do OH no estado fundamental permanece aproximadamente constante até 90 mm, o mesmo ocorrendo para o OH\*. Resultados similares para o OH fundamental foram obtidos pela técnica de LIF por Ribeiro, 2005. In this work, measurements in ethanol flames at different positions along the burner vertical axis were obtained, and for flow rates with equivalence ratios of 1.4, 1.0 e 0.8. The temperature values measured throughout a 55 mm distance above the burner varied from  $1905 \text{ K} \pm 64 \text{ K}$  to  $2238 \text{ K} \pm 155 \text{ K}$  for  $\phi = 1.5$ . Simulações feitas com o programa CHEMKIN-PREMIX mostraram uma tendência de variação da concentração de OH fundamental compatível com as obtidas neste trabalho.

Employing the GASEQ 0.79 software (Morley, 2005) and solving the problem for “adiabatic temperature and composition at constant pressure”, with rich products, the following results are obtained (initial temperature = 350 K):

$\phi = 2.4$	$T_{ad} = 2177 \text{ K}$	$[\text{OH}] = 0.057 \cdot 10^{-3} \text{ moles}$
$\phi = 1.8$	$T_{ad} = 2710 \text{ K}$	$[\text{OH}] = 2.6 \cdot 10^{-3} \text{ moles}$
$\phi = 1.5$	$T_{ad} = 2912 \text{ K}$	$[\text{OH}] = 8.7 \cdot 10^{-3} \text{ moles}$

These results are in agreement with that calculated from the images data (Fig 4): higher equivalence ratio gives flames with higher OH concentration. Further unidimensional CHEMKIN- PREMIX simulation will be performed to compare the results along the x-axis.

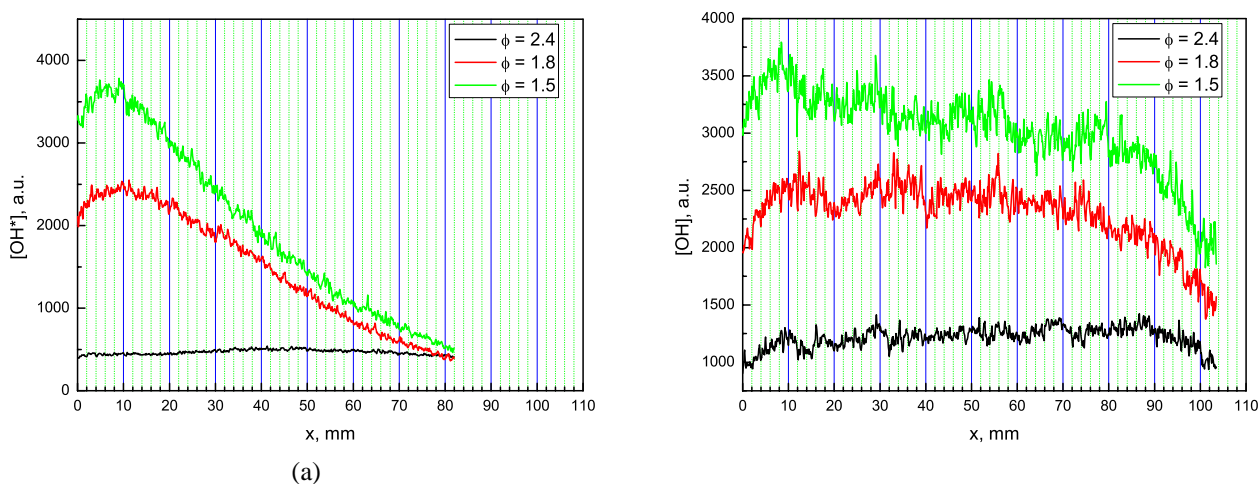


Figure 4. Downstream (x-axis) (a) OH\* chemiluminescent intensity distribution and (b) OH-LIF distribution, for the three studied premixed ethanol flames.

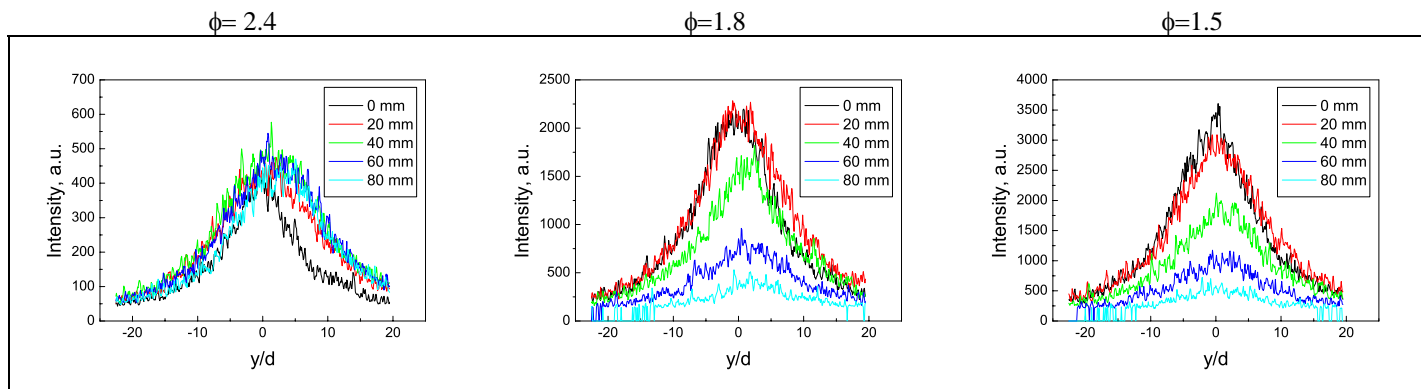


Figure 5. Radial OH\* radical distribution measured by emission imaging for the three studied flames at some height downstream the burner. The data are normalized in relation to the  $\phi = 1.5$  flame.

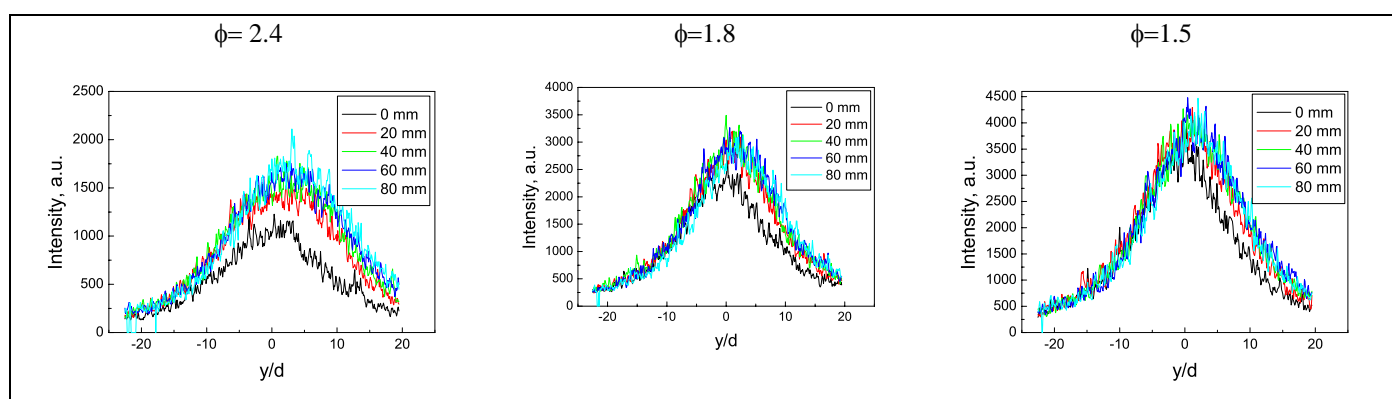


Figure 6. Radial OH radical distribution measured by PLIF imaging for the three studied flames at some height downstream the burner. The data are normalized in relation to the  $\phi = 1.5$  flame.

#### 4. CONCLUSION

OH\* radical emission and OH radical PLIF imaging were performed for three partially premixed vaporized ethanol/air/O<sub>2</sub> flames. The OH-PLIF flame distribution shows profiles larger than the OH\* radical distribution for the equivalent flames. As theoretical calculus demonstrate, the higher the flame equivalence ratio, the smaller the OH\* and OH radical concentrations. Almost homogeneous OH\* and OH radical distribution at the flame were found for the  $\phi = 2.4$  flame until 80 mm downstream the burner exit. For the  $\phi = 1.8$  and  $\phi = 1.5$  flames, the OH\* radical variation downstream the burner exit were more sensitive than that of the OH radical. Further CHEMKIN-PREMIX simulation needs to be performed to compare with the experimental data presented in this paper.

OH is an important radical in combustion studies because it is found in high concentrations at the reaction zone and also in the post-combustion gases. PLIF is a sensitive technique to study this radical.

#### 5. ACKNOWLEDGEMENTS

This research has been financially supported by the FAPESP (Fundação de Amparo à Pesquisa do Estado de São Paulo) and the CNPq (Conselho Nacional de Desenvolvimento Científico e Tecnológico).

#### 6. REFERENCES

- Bombac, R., Kappeli, B., 1999, "Simultaneous visualization of transient species in flames by planar-laser-induced fluorescence using a single laser system", *Appl. Phys. B*, Vol. 68, pp. 251-255.
- Dieke, G. H., Crosswhite, H. M., 1961, "The ultraviolet bands of OH", *J. Quant. Spectrosc. Radiat. Transfer*. Vol. 2, pp. 97-199.
- Eckbreth, A. C., 1988, "Laser Diagnostic for Combustion Temperature and Species," Abacus Press, Tunbridge Wells, UK.
- Gaydon, A. G., 1974 "Flame Structure and Reaction Processes. *The Spectroscopy of Flames*", John Wiley and Sons, New York, Chap. 5, pp. 266-273.

- Kee, R.J.; Rupley, F.M.; Miller, J.A.; Coltrin, M.E.; Grcar, J.F.; Meeks, E.; Moffat, H.K.; Lutz, A.E.; Dixon-Lewis, G.; Smooke, M.D.; Warnatz, J.; Evans, G.H.; Larson, R.S.; Mitchell, R.E.; Petzold, L.R.; Reynolds, W.C.; Caracotsios, M.; Stewart, W.E.; Glarborg, P.; Wang, C.; Adigun, O., 2000, *CHEMKIN Collection, Release 3.6*, Reaction Design, Inc., San Diego, CA.
- Lacava, P. T. (1995) Influência de Parâmetros de Atomização na Geração de Instabilidades Acústicas na Combustão de Sprays em Tubos Rijke, MSc Thesis, INPE, Cachoeira Paulista, SP, Brasil.
- Luque, J., Crosley, D. R., "Transition probabilities in the  $A^1\Sigma^+-X^2\Pi_i$  electronic system of OH", J. Chem. Phys., Vol.109. No. 2, pp. 439-448, 1998.
- Martins, C. A., Ferreira, M. A.; Pimenta, A. P.; Pires, A. C.; Carvalho Jr, J. A., 2005,. "CH And C<sub>2</sub> Radicals Characterization in natural gas turbulent diffusion flames". Revista Brasileira de Ciências Mecânicas, Brasil, v. XXVII, pp. 110-118.
- McManus, K., Yip, B., Candel, S., "Emission and Laser Induced Florescence Imaging Methods in Experimental Combustion", Exp. Therm. Fluid Sci., Vol. 10, pp. 486-512. 1995.
- Panoutsos<sup>1</sup>, C. S., Hardalupas<sup>1</sup> Y. \*, Taylor<sup>1</sup>, A.M.K.P. and Olofsson, J., Seyfried, H., M. Richter<sup>2</sup>, J. Hult<sup>2</sup>, M. Aldén Opt Lett 2003.
- Santos, L. R., "Medições de Temperaturas de Chamas de Etanol Utilizando Fluorescência Induzida por Laser", Thesis, 2005, 125 pp.
- Shirun Yang, Jianrong Zhao, Gong Yu, and Xinyu Zhang, Optical Technology and Image Processing For Fluids and Solids Diagnostics SPIE-Beijing 2002.
- Yang, S., Zhao, J., Yu. G., Zhang. X., 2002, Optical Technology and Image Processing For Fluids and Solids Diagnostics SPIE-Beijing.
- Morley, C., 2005, "Gaseq, Chemical Equilibria in Perfect Gases", version 0.76, < <http://www.arcl02.dsl.pipex.com> >.

## 7. RESPONSIBILITY NOTICE

The authors are the only responsible for the printed material included in this paper.